



马鞍山钢铁股份有限公司
MAANSHAN IRON & STEEL COMPANY LIMITED

2014 International Conference on Hot Stamping of UHSS

Investigation of Hot Stamping Process of 22MnB5 Based on Metallo-Thermo-Mechanical Theory

Liu Yonggang, etc.

Auto Sheet Strategic Business Unit, Maanshan Iron & Steel Co., Ltd., Maanshan, China

Aug. 20th 2014



Ed. by Li J.W.

Content

1

Introduction

2

Methodology

3

Numerical simulation

4

Results and analysis

5

Conclusions

1 Introduction

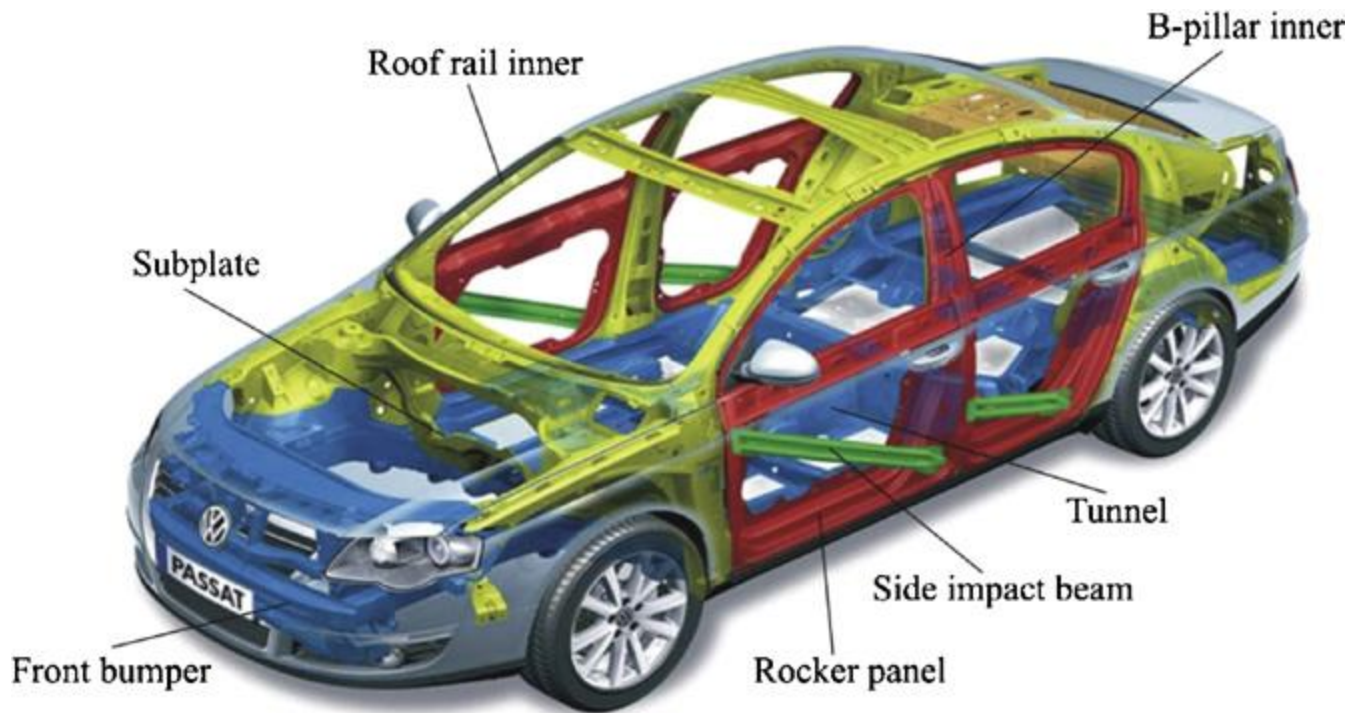


Fig.1 Hot stamped parts in a typical middle class car*

* Karbasian H, et al. *Journal of Materials Processing Technology*, 2010,210:2103-2118.

1 Introduction

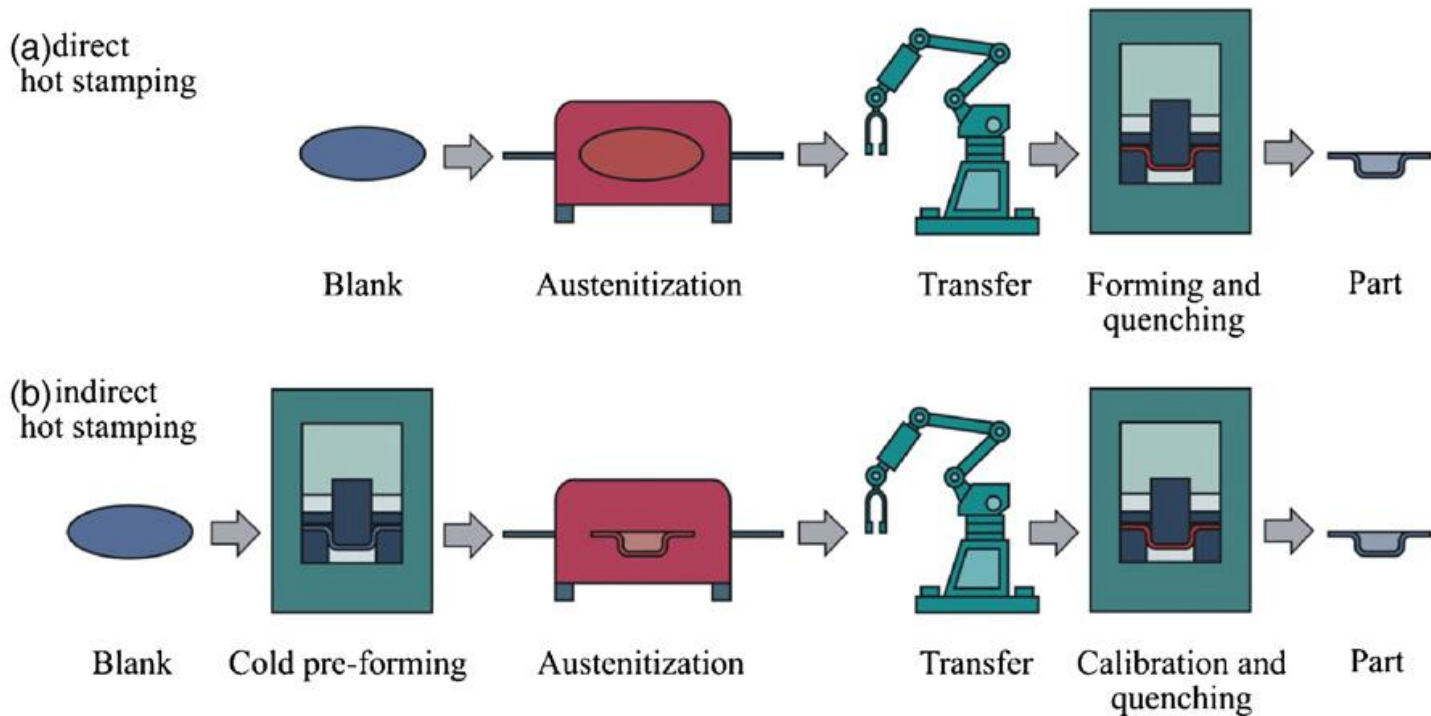


Fig.2 Basic hot stamping process chains: (a) direct hot stamping, (b) indirect hot stamping.*

* Karbasian H, et al. *Journal of Materials Processing Technology*, 2010,210:2103-2118.

1 Introduction

Hot stamping processing

- First, the high-strength steel sheet is heated in the furnace to **achieve full-austenitic transformation**.
- Subsequently experience the **forming process**
- Finally, **quenching** in forming die equipped with a cooling system to ensure that cooling rate is greater than the critical value of **27°C /S**.

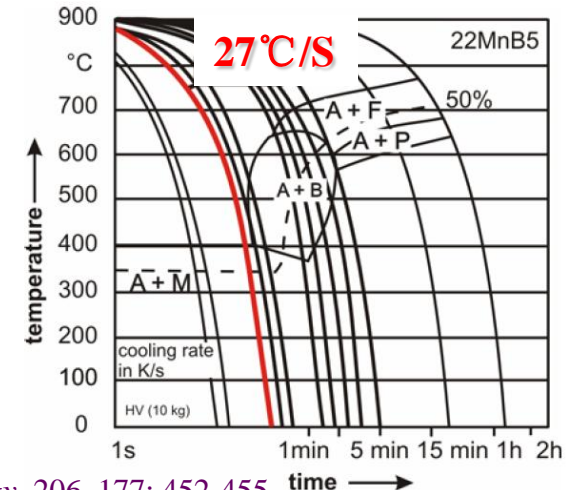


Fig.3 The CCT diagram of 22MnB5.*

* Merklein M, et al. *Journal of Materials Processing Technology*, 206, 177: 452-455.

1 Introduction

- Recently, a great many of previous researches only have taken the phase transformation and the mechanical properties into account for hot stamping analyses, but **ignoring the effect of cooling water** *.
- In this paper, **considering the cooling system**, hot stamping process of a 22MnB5 box component is simulated based on the **metallo-thermo-mechanical theory** to discuss the **temperature and microstructure evolution rule**, and analyze the influences of holding time on the mechanical properties and final microstructure distribution of component.

* Cui J, *et al. Journal of Materials Engineering and Performance*, 2012, 21: 2244–2254.

* Xing Z W, *et al. Materials Science and Engineering A*, 2009, 499: 28-31.

2 Methodology

- Hot stamping process is a complex multi-field problem involving the reciprocal coupling among the thermal, metallurgical and mechanical fields.

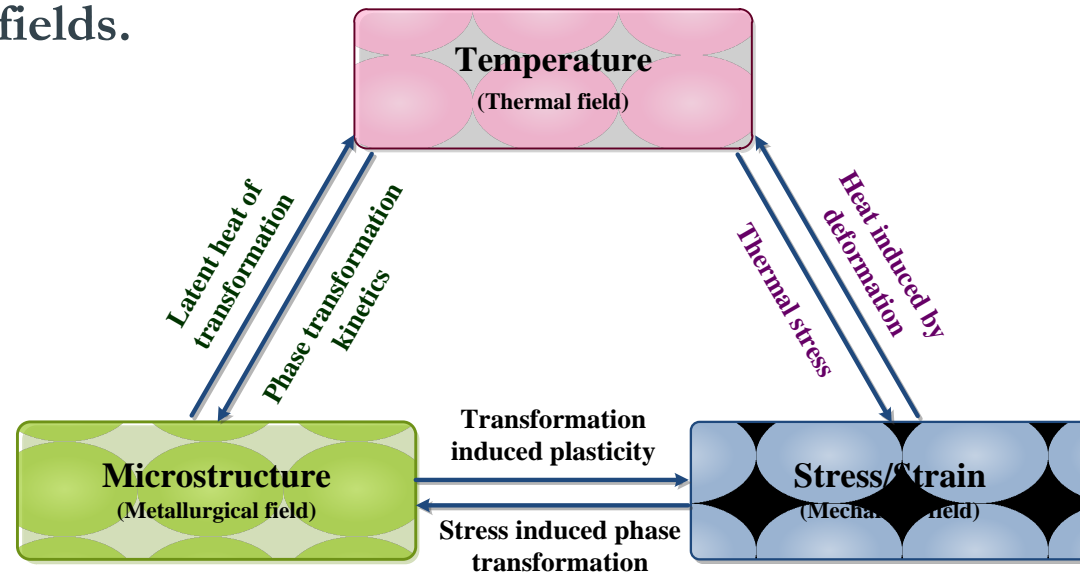


Fig.4 Illustration of the metallo-thermo-mechanical coupling relationship in hot stamping process.*

* Caner Simsir, *et al. Computational Materials Science*, 2008, 44: 588-600.

* T Inoue, K Arimoto. *Journal of Materials Engineering and Performance*, 1997, 6: 51-60.

2 Methodology

Temperature model

- Fourier's law *
$$\rho c \frac{\partial T}{\partial t} = \frac{\partial}{\partial x} \left(\lambda \frac{\partial T}{\partial x} \right) + \frac{\partial}{\partial y} \left(\lambda \frac{\partial T}{\partial y} \right) + \frac{\partial}{\partial z} \left(\lambda \frac{\partial T}{\partial z} \right) + Q$$

- Initial condition
$$T|_{t=0} = T_0(x, y, z)$$

- Boundary condition
$$-\lambda \frac{\partial T}{\partial n} \Big|_r = H_c (T_B - T_E) + H_R (T_B^4 - T_E^4)$$

- H_c and H_R are the convection and radiation heat transfer coefficients

* Caner Simsir, *et al. Computational Materials Science*, 2008, 44: 588-600.

2 Methodology

Phase transformation model

- Diffusional controlled transformations*

For *Ferrite*, *Pearlite* and *Bainite* transformation

$$n = \frac{\ln[\ln(1-\xi_1)/\ln(1-\xi_2)]}{\ln(t_1/t_2)}$$

$$\xi = 1 - \exp(-bt^n)$$

$$b = -\frac{\ln(1-\xi_1)}{t_1^n}$$

- b and n are constants, which can be confirmed by isothermal transformation (TTT) diagram.

* Caner Simsir, *et al. Computational Materials Science*, 2008, 44: 588-600.

2 Methodology

Phase transformation model

- Non-diffusional controlled transformations*

For *martensite* transformation

$$\xi = 1 - \exp[-\alpha(M_s - T)]$$

- M_s is martensitic point.
- α is constant.

* Koistien D F, *et al. Acta Metallurgica*, 1959, 7: 50-60.

2 Methodology

Stress/strain model

- Fourier's law $\bar{\sigma} = K(\bar{\varepsilon}_0 + \bar{\varepsilon})^n \dot{\bar{\varepsilon}}^m e^{(\beta/T)}$

- Strain increment *

$$\dot{\bar{\varepsilon}} = \dot{\bar{\varepsilon}}_e + \dot{\bar{\varepsilon}}_p + \dot{\bar{\varepsilon}}_{th} + \dot{\bar{\varepsilon}}_{pt} + \dot{\bar{\varepsilon}}_{tp}$$

- **Elastic** rate
- **Plastic** rate
- **Thermal** rate
- **Phase transformation** rate
- **Transformation plasticity** rate

* Arif Sugianto, *et al. Journal of Materials Processing Technology*, 2009, 209: 3597-3609.

2 Methodology

Hardness prediction model

- Maynier model*

$$HV = \xi_M HV_M + \xi_B HV_B + (\xi_P + \xi_F) HV_{F-P}$$

$$\xi_M + \xi_B + \xi_P + \xi_F = 1$$

$$HV_M = 127 + 949C + 27Si + 11Mn + 8Ni + 16Cr + 21 \log V_r$$

$$HV_B = 323 + 185C + 330Si + 153Mn + 65Ni + 144Cr + 191Mo \\ + (89 + 53C - 55Si - 22Mn - 10Ni - 20Cr - 33Mo) \log V_r$$

$$HV_{F-P} = 42 + 223C + 53Si + 30Mn + 12.6Ni + 7Cr + 19Mo \\ + (10 - 19Si + 4Ni + 8Cr + 130V) \log V_r$$

* P Maynier, *et al. Hardenability concepts with applications to steels*, AIME, New York, NY, 1978.

3 Numerical simulation

Geometry

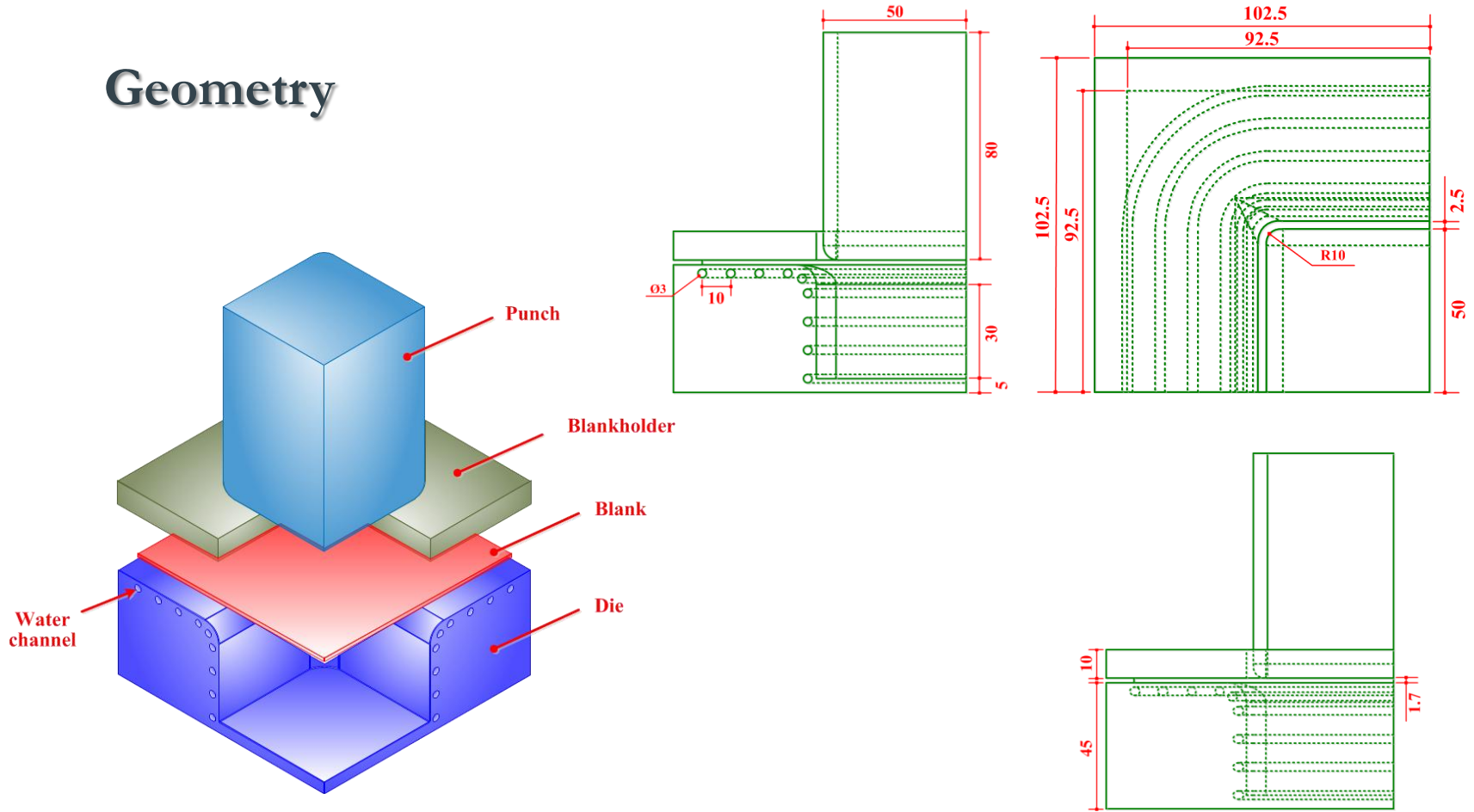
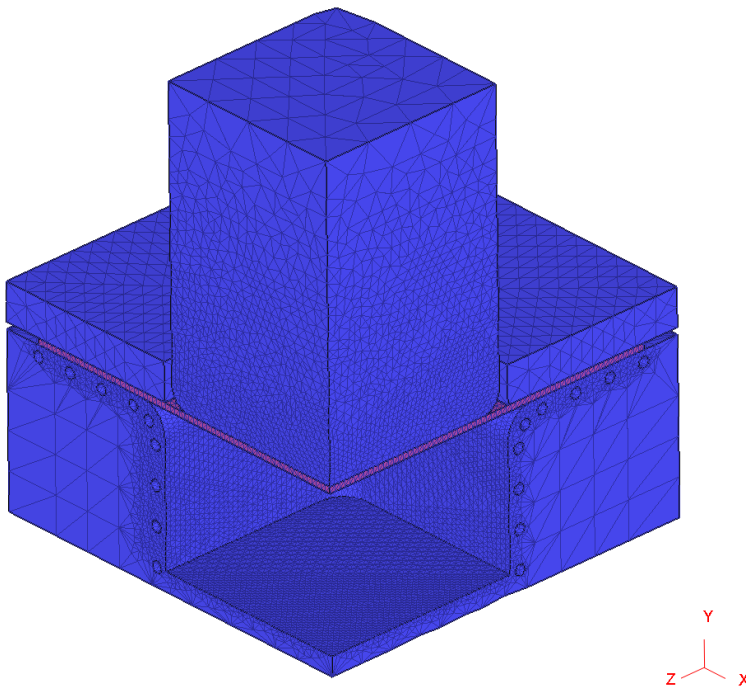


Fig.5 Geometry and dimension for hot stamping simulation.

3 Numerical simulation

FEM model



- The velocity of water is 3.5m/s considered with a convective heat transfer coefficient of $15000\text{w}/(\text{m}^2\cdot\text{K})$.
- The **brick and tetrahedral elements** are used to discretize the blank and tools, respectively.
- The numbers of nodes and elements of **tools** are **55458** and **263932**, while that of **blank** are **4418** and **2116**.

Fig.6 FEM model for hot stamping simulation.

3 Numerical simulation

Hot stamping process

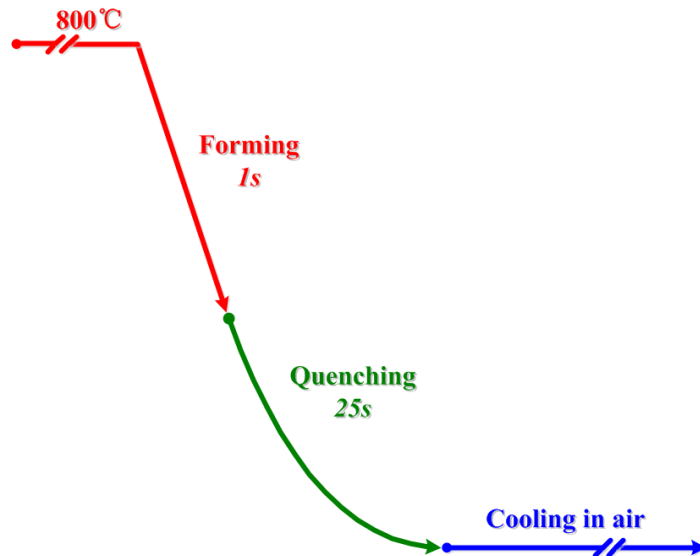
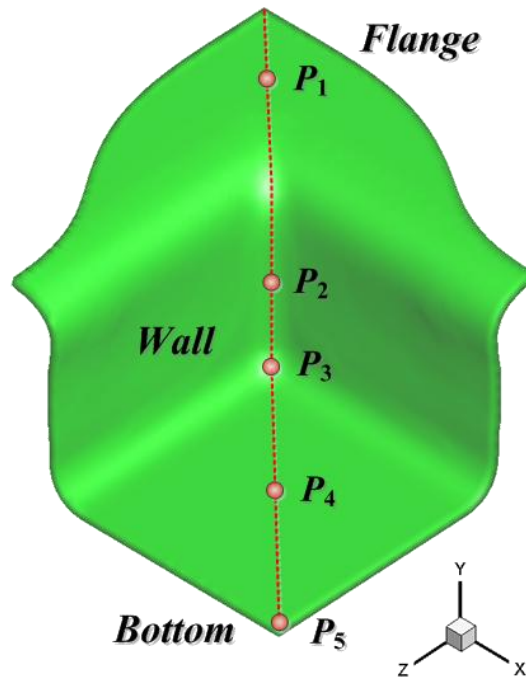


Fig.7 Illustration of hot stamping process.

- Firstly, the hot blank is **transferred** to the punching machine and formed.
- Subsequently, the forming component is **holding** in die for few seconds to make the microstructure of blank change into martensite completely.
- Finally, the component is ejected from the die and **cooled by air**.
- The initial temperatures of boron steel blank and tools are assumed as **800 °C and 25 °C**, respectively.

4 Results and analysis

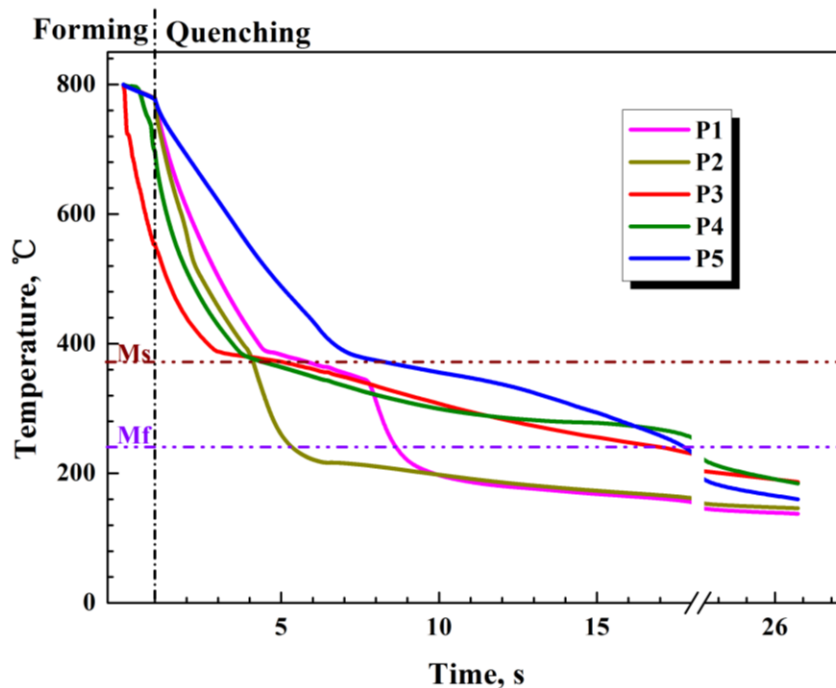
Temperature evolution



- Five tracking points located in the **flange**, **wall** and **bottom** of box component (namely, **P₁**, **P₂**, **P₃**, **P₄** and **P₅**) are selected to monitor the temperature, microstructure evolution and hardness distribution during hot stamping process

4 Results and analysis

Temperature evolution



- At the forming process, due to the direct contact between the blank and punch, **P3 demonstrates a sharply decrease**, while the temperature drop of other points is more gently.
- **After 1s**, the forming process is completed and entered the quenching process in die.
- About **3s later**, **P3 firstly occurs the martensitic phase transformation**.
- Approximate **16s**, all points has been **achieve the martensitic finish temperature (Mf)** and the component can be ejected and cooled by air.

Fig.8 Time-dependent temperature curves of box component at different tracking points during hot stamping process.

4 Results and analysis

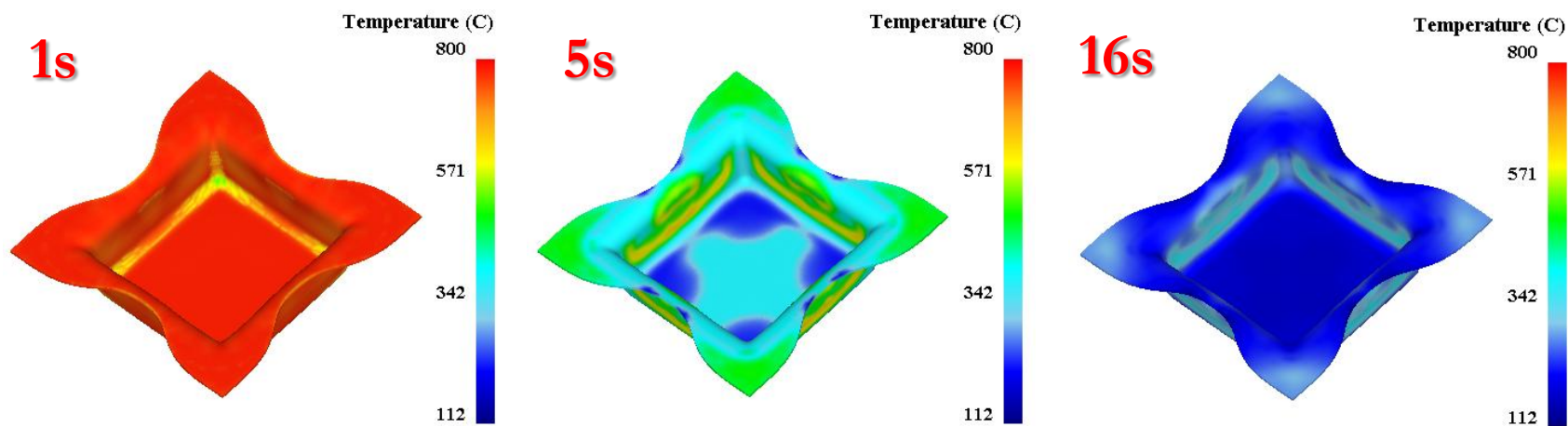


Fig.9 Temperature distribution of box component at different time.

4 Results and analysis

- After forming, the temperature at the **bottom and flange** almost uniformly (**about 800°C**), while at the **bottom corner** the lowest temperature is **nearly 560 °C**.
- The contact condition had a significant influence on the temperature distributions.
- The gap between the blank and die causes a remarkable increase of heat exchange velocity.
- During quenching, the temperature of component decreases evidently and the **maximum cooling rate takes place at the bottom**.
- After **quenching for 16s**, the temperature of the entire component is **lower than Mf** and with **a continuous uniform distribution**.

4 Results and analysis

Microstructure evolution

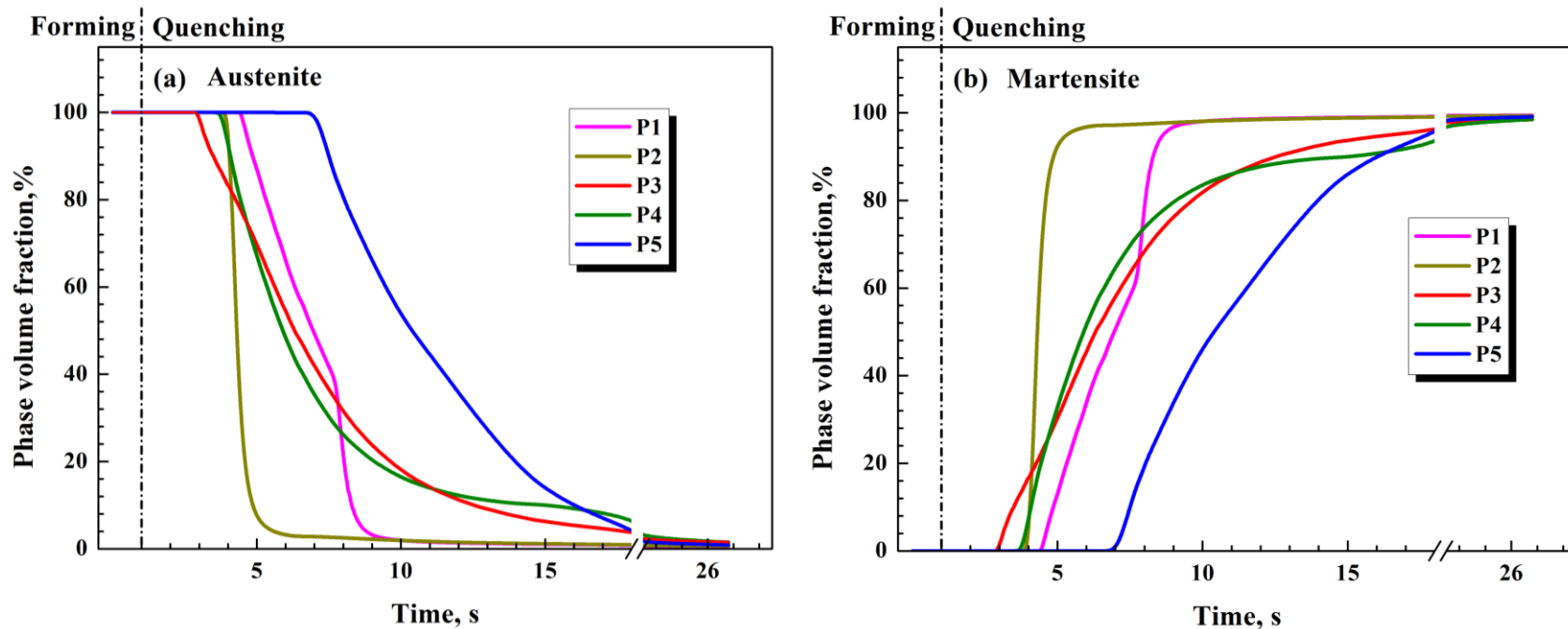


Fig.10 (a) Austenite and (b) martensite volume fractions of box component at different tracking points during hot stamping process.

4 Results and analysis

- **After forming**, the microstructure of component is still composed **almost entirely of austenite**.
- When the holding times have been enlarged to about **6s** and **9s**, the **phase transformation from austenite to martensite** at tracking points **P2 and P1 are fully completed**, respectively, while other tracking points need to last longer.
- After about **16s**, the austenite volume fraction of component has been significantly decreased and finally its volume fraction is below 10%, while the **martensite volume fraction has already gone beyond 90%**.

4 Results and analysis

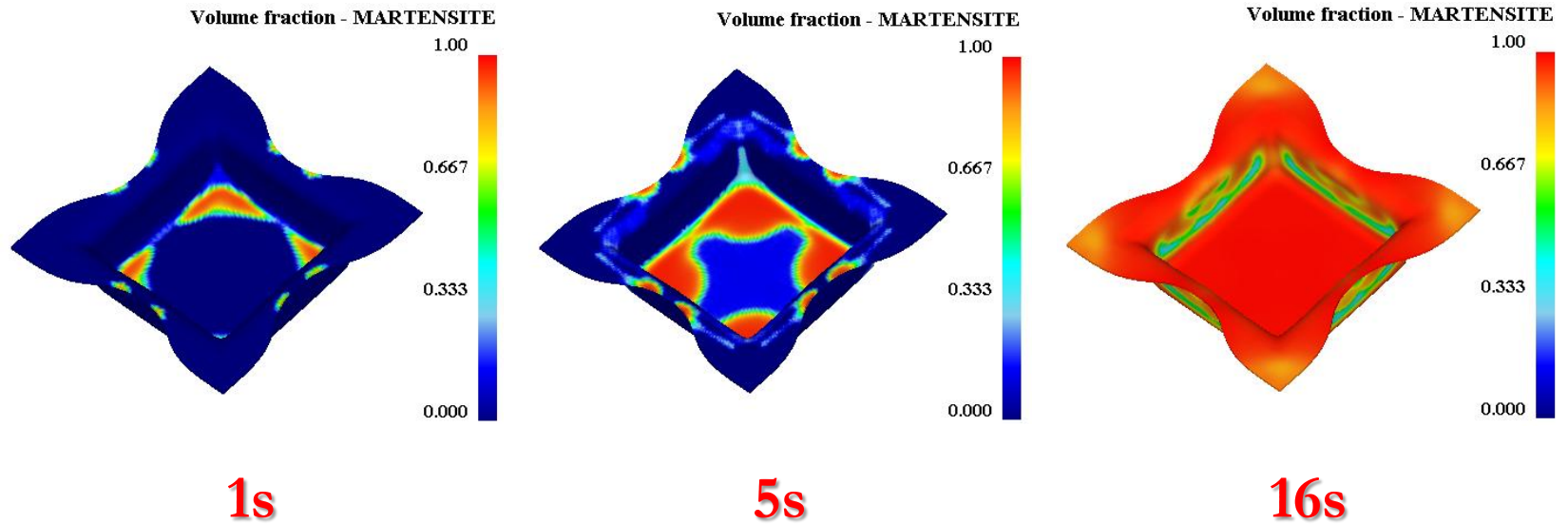


Fig.11 Microstructure distribution of box component at different time.

4 Results and analysis

- Phase transformation from **austenitic to martensite first takes place at the bottom corner** of the formed component and subsequently progresses rapidly to the bottom and flange of component, which is in accord with the temperature evolution in formed component.
- The martensite volume fraction of component increases with the extension of holding time. When the time increases to **16 s, most of austenite has transformed into martensite.**
- In contrast, the content of **martensite at the wall of component is relatively lower**, but the certain area in the **wall with the minimum amount of martensite is also more than 60%.**

4 Results and analysis

Hardness distribution

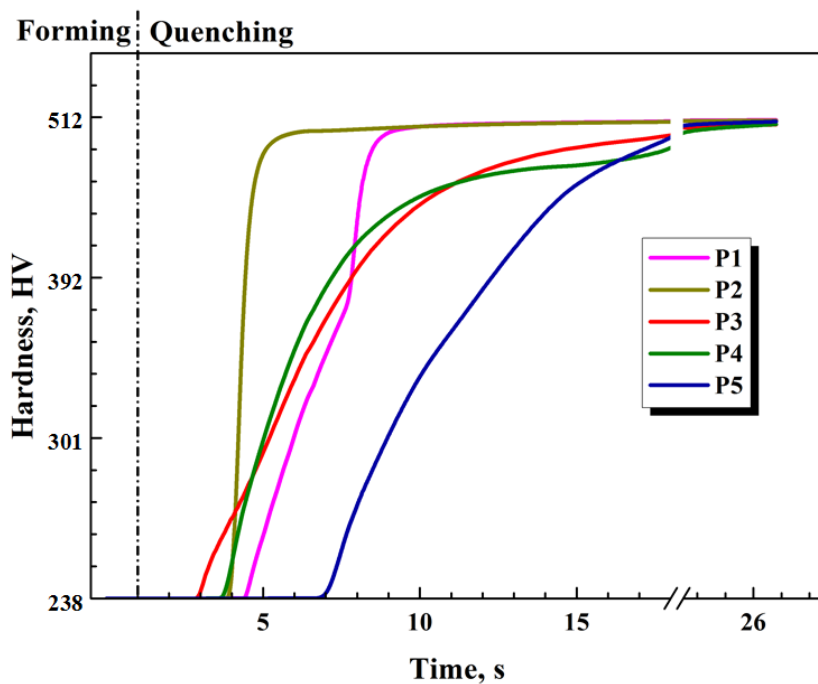


Fig.12 Hardness curves of box component at different tracking points during hot stamping process.

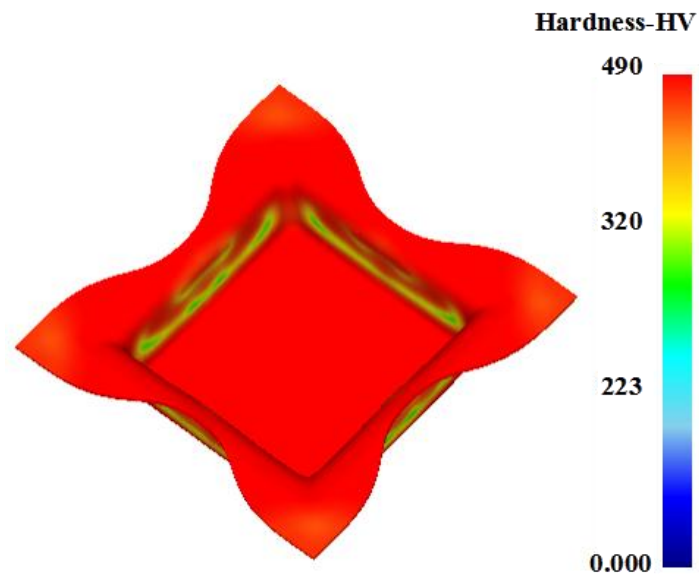


Fig.13 Hardness distribution of box component after hot stamping for 16s.

4 Results and analysis

- **To satisfy the required hardness**, the sufficient holding time of quenching in die is essential .
- As the holding time increases, the hardness in various regions of component shows a similar and distinct increasing trend. The predicted hardness of component after hot stamping is **almost 512HV**.
- After hot stamping for **16s**, the **hardness in the wall of component is lower** than those in other locations due to its slower cooling rate.
- Except the wall of component, **the component obtains a nearly uniform hardness of 500HV** at the bottom and flange in the current cooling time.

5 Conclusions

- Considering the cooling system, the hot stamping process of 22MnB5 box component is successfully reproduced based on the metallo-thermo-mechanical theory, which can **provide a theoretical guidance for optimizing the hot stamping procedure.**
- To satisfy the required mechanical properties of formed component, **the sufficient holding time of quenching in die is essential** and it plays an important role in ensuring the required hardness.
- The predicted hardness of component after stamping is almost 512HV and it **shows a good agreement with the experimental results.**

2014 International Conference on Hot Stamping of UHSS



Thank you!

- ❖ **Liu Yonggang PH. D.**
- ❖ **Auto Sheet Strategic Business Unit Maanshan Iron & Steel Co.,Ltd., Maanshan, China**
- ❖ **Add.: CiHu New District, Maanshan City, Anhui Province, China**
- ❖ **Tel.: 0555-2871101**
- ❖ **Fax: 0555-x2871101**
- ❖ **E-mail: lyghotmail@hotmail.com**